

Reaction Calorimetry as a New Tool for Supercritical Fluids

Frédéric Lavanchy, Sophie Fortini, and Thierry Meyer*

Institute of Chemical and Biological Process Science, Swiss Federal Institute of Technology, 1015 Lausanne, Switzerland

Abstract:

Reaction calorimetry is an efficient tool used to obtain kinetic, thermodynamic, and safety data. A new tool, composed of a high-pressure reactor (HP350) coupled with a Mettler-Toledo RC1e reaction calorimeter, is developed for the investigation of chemical reactions, under supercritical conditions. The reactor ($V = 1.2$ L) can be pressurized up to 350 bar and heated to 300 °C. Results presented in this contribution are divided into three sections. The first part concerns some highlights of the technical challenge related to supercritical reaction calorimetry in comparison with the classical liquid calorimetry. The second part presents a Wilson plot analysis with pure supercritical CO₂ and shows that, in contrast to classical liquids, the lower the temperature (above the critical point) the better the heat transfer coefficient. This tendency can be explained by the evolution of scCO₂ thermodynamical and transport properties around the critical point. The third part contains preliminary results from the dispersion polymerization of methyl methacrylate in supercritical carbon dioxide using poly(dimethylsiloxane) macromonomer as stabilizer. Poly (methyl methacrylate) can be produced with high yield, high molecular weight, and narrow particle size distribution, using 10 wt % (with respect to monomer) stabilizer under efficient stirring. A polymerization enthalpy of -58.8 ± 3 kJ/mol has been calculated with high reproducibility, being in good agreement with previously reported data. This confirms that the employed heat balance model is correct and shows the important potential of reaction calorimetry for the promotion of supercritical fluid technologies at industrial scale, since it allows the determination of kinetics, thermodynamic, and safety data.

Introduction

Supercritical fluids (SCFs) show very specific properties that lie between those of a gas and those of a liquid. This particularity is one reason for their great interest, as by varying pressure or temperature, properties such as product solubility can be tuned to accelerate the separation as density has been changed from gas to liquid one.¹ At pressures and temperatures near the critical point, spectacular changes in specific properties occur, which are fundamental for the understanding of supercritical fluids behaviour. The most widely used SCF is carbon dioxide (scCO₂), which has tunable properties with pressure and temperature, has low critical pressure and temperature, respectively 73.9 bar and 31 °C, is nontoxic, nonflammable, and environmentally friendly. It could be suitable for organic solvents replacement

in chemical processes, especially extraction processes, due to its high diffusion rates.²

However, industrial applications of supercritical fluids are scarce, and only few reactive processes have been effectively developed. In the future, the need to replace organic solvents will increase not only for environmental reasons but to benefit from new productive routes.³ For SCFs a financial balance has to be made to evaluate the process viability, keeping in mind that infrastructure and energy costs for gas compression are very strong limitations. An example of an economical study is given by Hâncu and Beckmann with the system anthraquinone/anthrahydroquinone in sub- and supercritical CO₂.⁴

Reaction calorimetry is a common tool to investigate chemical reaction kinetics, to determine required data for chemical process safety, and to access fundamental information about phase changes. The advantage of working at larger scale is that, in contrast to small-scale batch or tubular cells calorimeter (1–10 cm³), effects of mixing, heat conduction, and heat transfer can be investigated additionally. Until now, very few publications deal with calorimetry applied to supercritical phase and the results presented in this report describe, to our knowledge, the first development and use of a reaction calorimeter for supercritical field applications.⁵ In particular, heat transfer in scCO₂ will be emphasized.

The increasing interest over the last few decades in decreasing the release of organic compounds (VOCs) and aqueous wastes has motivated the development of conducting polymerization reactions in supercritical carbon dioxide.⁶ Moreover, there is no chain transfer to CO₂ in free radical polymerizations. Generally, monomers exhibit good solubility in CO₂. However, CO₂ is a rather poor solvent for most high-molecular weight polymers except for some fluoropolymers and silicones.⁷ The latter are used as sterical stabilizers in the dispersion polymerization of vinyl polymers such as poly(methyl methacrylate)^{8,9} and poly(styrene).¹⁰

The dispersion polymerization of methyl methacrylate in supercritical carbon dioxide, using the commercially available

- (2) Poliakoff, M.; Howdle, S. M.; George, M. W.; Han, B.-X.; Yan, H.-K.; Bagratashvili, V. N. *Chin. J. Chem.* **1999**, *17*, 212.
- (3) Sherman, J.; Chin, B.; Huibers, P. D. T.; Garcia-Valls, R.; Hatton, T. A. *Environ. Health Perspect.* **1998**, *106*, 253.
- (4) Hancu, D.; Beckman, E. J. *React. Eng. Pollut. Prev.* **2000**, 191.
- (5) Lavanchy, F.; Fortini, S.; Meyer, T. *Chimia* **2002**, *56*, 126.
- (6) Cooper, A. I. *J. Mater. Chem.* **2000**, *10*, 207.
- (7) Cooper, A. I.; DeSimone, J. M. *Curr. Opin. Solid State. Mater. Sci.* **1996**, *1*, 761.
- (8) O'Neill, M. L.; Yates, M. Z.; Johnston, K. P.; Smith, C. D.; Wilkinson, S. P. *Macromolecules* **1998**, *31*, 2838.
- (9) O'Neill, M. L.; Yates, M. Z.; Johnston, K. P.; Smith, C. D.; Wilkinson, S. P. *Macromolecules* **1998**, *31*, 2848.
- (10) Canelas, D. A.; Betts, D. E.; DeSimone, J. M. *Macromolecules* **1996**, *29*, 2818.

* To whom correspondence should be addressed. E-mail: thierry.meyer@epfl.ch.

(1) Kiran, E.; Debenedetti, P. G.; Peters, C. J. *NATO Sci. Ser.* **2000**, *366*, 596.



Figure 1. Autoclave.

poly(dimethylsiloxane) monomethacrylate (PDMS macromonomer) as dispersant,¹¹ is used as model reaction. Preliminary results presented will serve not only to validate the heat transfer model developed for supercritical fluid applications but also to illustrate the great potential of reaction calorimetry as a thermo-analytical tool.

The Supercritical Reaction Calorimeter

In collaboration with Mettler-Toledo GmbH, the reaction calorimeter has been developed for supercritical conditions, using a high-pressure stainless steel reactor HP350 (Premex, Switzerland), presented in Figure 1.

The maximum operating pressure and temperature are 350 bar and 300 °C, respectively. The reactor is equipped with a magnetic drive, a 25-W calibration heater, a PT100 temperature sensor, and a pressure sensor. The stirrers used are a three-stage Ekato MIG and a two-stage turbine (Figure 2a and b, respectively).

The reactor, with a total volume of 1.2 L (V_r), is surrounded by a jacket where silicon oil flows at high flow rate. The thermostat unit controls the reaction temperature by pumping silicon oil through the double jacket of the reactor. A technical scheme of the installation is given in Figure 3.

The calorimeter is able to work in three different operating modes: *adiabatic*, where the jacket temperature (T_j) is adjusted in such a manner that there is no heat transfer through the reactor wall; *isoperibolic*, where the jacket temperature is kept constant and the reaction temperature (T_r) follows the reaction profile; and *isothermal*, where the desired reaction temperature is set to a constant value and T_j is changed automatically to maintain T_r at the specified value. All the experiments presented in this contribution are performed using the isothermal mode.

The Technical Challenge. The so-called “supercritical reaction calorimetry” first has to overcome some technical

problems simply due to the fact that the supercritical phase occupies all available space as illustrated in Figure 4. Thus, not only the jacket area has to be perfectly controlled but also the cover and the other parts have to be separately temperature controlled for the heat balance equations to be applied without any additional heat transfer interferences. In our case, all the reactor parts in contact with the reacting media are adjusted to T_r to neglect the heat accumulation term.

Heat Balance Equations. The most fundamental assumptions are that reactor and jacket temperature are homogeneous, and that the reaction system is perfectly mixed. The energy balance for a semi-batch process is given by:

$$Q_r + Q_c = Q_{acc} + Q_{dos} + Q_{flow} + Q_{loss} - Q_{stir} \quad (1)$$

where Q_r is the heat generation of the reaction, [W]. Q_{acc} is the accumulation term, [W]. Q_c is the heat delivered by the calibration probe, [W]. Q_{dos} corresponds to the amount of heat due to addition of reactants, [W]. Q_{flow} is the heat flow through the reaction wall, [W]. Q_{loss} is the heat losses to the surroundings, [W], Q_{stir} being the heat dissipated by the stirrer, [W].

The heat release by a polymerization reaction is defined by the eq 2, where $V_{continuousphase}$ is the total volume of the reactor in this case, V_r , [m³]; $(-\Delta H_r)$ is the heat of polymerization of the monomer used [J/mol]; and R_p is the global rate of polymerization [mol/(m³·s)].

$$Q_r = V_{continuousphase} \cdot (-\Delta H_r) \cdot R_p \quad (2)$$

The accumulation term Q_{acc} defined by eq 3 corresponds to the heat needed to change the internal temperature T_r [K] of the media by a certain amount dT_r/dt [K/s]. m_r is the reaction mass [kg], c_{pr} the specific heat capacity of the reaction mass [J/(kg·K)] and C_{pi} is the heat capacity of each insert, [J/K]. This term can be neglected as soon as the system is working in a pure isothermal mode. Equation 3 does not include the accumulation term for the reactor itself as it is compensated for in the WinRC software by the use of a corrected jacketed temperature.

$$Q_{acc} = (m_r \cdot c_{pr} + \sum_i C_{pi}) \cdot \frac{dT_r}{dt} \quad (3)$$

The calibration probe delivers an amount of heat Q_c that is measured on-line and has a value around 25 W. It is used to measure the overall heat transfer coefficient, UA , either during Wilson plot experiments or before and after reactions according to eq 4. Calibration runs during 10 min at constant internal temperature T_r .

$$UA = \frac{\int_{t_1}^{t_2} (Q_c - Q_b) \cdot dt}{\int_{t_1}^{t_2} (T_r - T_j) \cdot dt} \quad (4)$$

Q_b is the baseline term, which will be discussed later, and T_j is the jacket temperature [K].

The dosing term, defined in eq 5, is the amount of heat absorbed or released due to the reactant addition at a

(11) Giles, M. R.; Hay, J. N.; Howdle, S. M.; Winder, R. J. *Polymer* **2000**, *41*, 6715.



Three-stage Ekato MIG®



Two-stage Turbine

Figure 2. (a) Three-stage Ekato MIG. (b) Two-stage turbine.

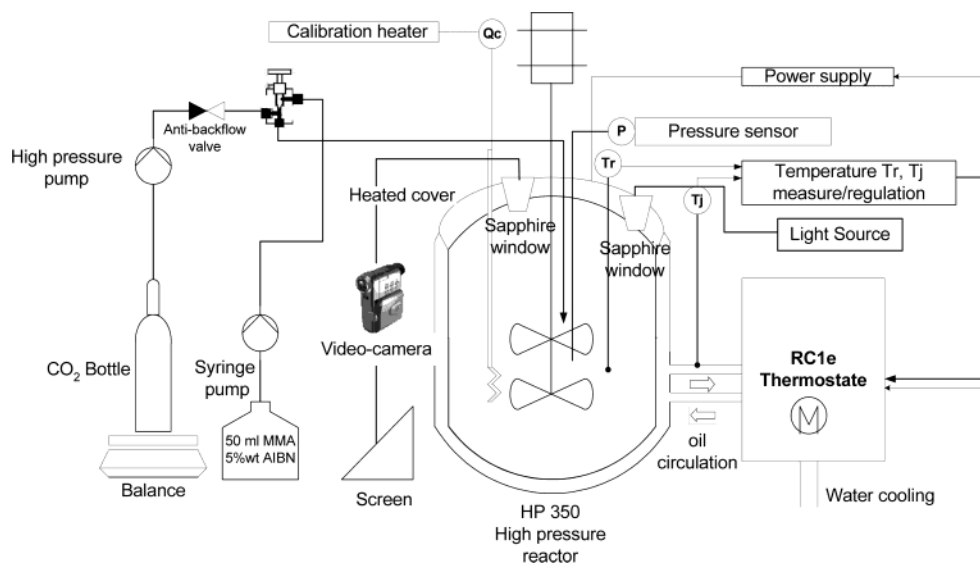


Figure 3. Technical scheme of the RC1e unit and the additional equipment.

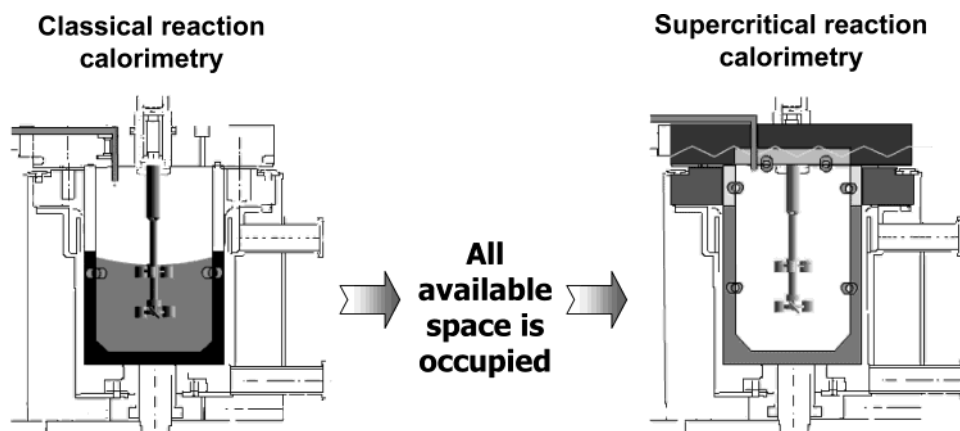


Figure 4. Difference between classical liquid and supercritical reaction calorimetry.

different temperature than the reaction mass:

$$Q_{\text{dos}} = \frac{dm_d}{dt} \cdot c_{\text{pd}} \cdot (T_r - T_{\text{dos}}) \quad (5)$$

where dm_d/dt is the mass flow of dosing [kg/s]; c_{pr} is the specific heat of the added substance [J/(kg·K)]; T_r is the current temperature of the reactor contents [K]; T_{dos} is the temperature of the added substance. It has been observed

during all the presented isothermal experiments that the dosing term can be neglected due to the small quantity of reactant added.

The term Q_{flow} in eq 1 is the heat flow through the reactor wall:

$$Q_{\text{flow}} = U \cdot A \cdot (T_r - T_j) \quad (6)$$

where U is the overall heat transfer coefficient [W/(m²·K)]

and A is the heat exchange surface [m^2]. As soon as the supercritical fluid occupies all the volume available, the heat exchange area corresponds to its maximum geometrical value.

The two terms Q_{loss} and Q_{stir} in eq 1 are normally constant during an isothermal run and can be combined in the baseline term Q_b . This means that the integration of a heat production or a calibration peak already takes into account heat losses and the heat dissipated by stirring as soon as stirrer speed and temperature do not change. However, the measure of UA before and after the reaction taking into account a constant baseline (Q_b) are sufficient for reactions with only small changes of physicochemical properties. For polymerizations, this assumption is limited as the viscosity can change significantly during the process. Thus, the two terms Q_{stir} and UA , which are directly dependent on the media viscosity, can evolve during the polymerization process.

From eqs 1 and 2 it can be seen that the reaction rate is related to the evolution of the measured heat. For single reactions or one dominant reaction, such as the propagation reaction in free radical or chain polymerization processes, Q_r is directly proportional to the measured heat. For complex systems, where consecutive or parallel reactions with similar thermal contributions occur, the signal corresponds to the addition of all heat contributions, i.e., the macrokinetic. The final and simplified heat balance equation used in this report for the polymerization part is given in eq 7 and takes into account all the previous remarks:

$$Q_r = Q_{\text{flow}} \quad (7)$$

Internal Heat Transfer. Wilson plot analysis combines two expressions.¹² The first expression concerns the global heat transfer resistance $1/U$ being expressed as the sum of three resistances: one from the internal film h_r , one for the jacket wall, and one from the external oil coolant film h_{oil} . The last two are combined in a global resistance expression $1/\varphi$ being independent of the internal media (eq 8). The second expression is the dimensionless “Nusselt correlation” relating Nusselt number (Nu) to Reynolds (Re) and Prandtl (Pr) numbers (eq 9).

$$\frac{1}{U} = \frac{1}{h_r} + \frac{e}{\lambda_w} + \frac{1}{h_{\text{oil}}} = \frac{1}{C' \cdot N^{2/3}} + \frac{1}{\varphi} \quad (8)$$

$$Nu = C \cdot Re^a \cdot Pr^b \left(\frac{\mu}{\mu_w} \right)^c = \frac{h_r \cdot d_R}{\lambda} = C \cdot \left(\frac{N \cdot d_S^2 \cdot \rho}{\mu} \right)^a \cdot \left(\frac{c_p \cdot \mu}{\lambda} \right)^b \left(\frac{\mu}{\mu_w} \right)^c \quad (9)$$

where h_r is the internal heat transfer coefficient, [$\text{W}/(\text{m}^2 \cdot \text{K})$], e is the thickness of the metallic wall, [m], λ_w is the heat conductivity of the metallic wall, [$\text{W}/(\text{m} \cdot \text{K})$], h_{oil} is the coolant part heat transfer coefficient, [$\text{W}/(\text{m}^2 \cdot \text{K})$], d_R is the reactor internal diameter, [m], λ is the bulk heat conductivity, [$\text{W}/(\text{m} \cdot \text{K})$], μ is the bulk dynamic viscosity, [$\text{kg}/(\text{m} \cdot \text{s})$], N is the rotation speed of the stirrer, [s^{-1}], d_S is the stirrer characteristic diameter, [m], ρ is the bulk density, [kg/m^3], c_p is the bulk constant pressure heat capacity,

[$\text{J}/(\text{kg} \cdot \text{K})$], C and C' are constants. The exponent a for the Reynolds number in the Nusselt expression is usually $2/3$ for a stirred tank reactor equipped with a turbine in liquid media.¹³ Exponent b for the Prandtl number is $1/3$. The viscosity ratio, for which exponent c is usually 0.14 , is neglected since the maximum temperature difference between the bulk μ and the wall μ_w is less than 1°C in the isothermal mode.

This allows the isolation of h_r and its substitution in the resistance expression as all other properties are constant at isothermal conditions.

Experimental Section

Carbon dioxide of purity 99.9% is supplied by Carbagaz (Switzerland). The bottle is mounted on a balance (Mettler-Toledo GmbH, Switzerland) with an extended precision of 0.1 g over the range of $0\text{--}12.8 \text{ kg}$ and is connected to a CO_2 pump equipped with a cooling chamber to pump liquid CO_2 (NWA GmbH, Germany).

The typical Wilson experiments procedure consists of the following: The reactor is filled two times with about 50 g of CO_2 , is emptied through the purging valve, and then is continuously purged by CO_2 flowing. The valve is then closed, and the reactor is filled up to a given mass using the pump. The valve is then closed again, and a 10-min stabilization time is systematically applied before noting the total injected CO_2 mass. Eight stirrer speeds between 100 and 2000 rpm have been tested with the two-stage turbine and the three-stage Ekato MIG for four isotherms: 32 , 35 , 50 , 100°C and different densities.

The dispersion polymerization of methyl methacrylate in scCO_2 using poly(dimethylsiloxane) macromonomer as stabilizer is realized using the following products: the stabilizer (PDMS macromonomer, $\text{MW} \approx 5000 \text{ g/mol}$) is supplied by ABCR (Germany), the initiator (2,2'-azobis(isobutyronitrile), AIBN) is supplied by Fluka, and the monomer (methyl methacrylate, MMA) is supplied by BASF (Germany). All components are used without further purification.

The polymerization reaction procedure is the following: the reaction vessel is charged with monomer (200 g) and the required amount of stabilizer and then closed and filled with CO_2 (around 800 g). The temperature is raised to 80°C . At this temperature, a 50-mL MMA solution containing $5.1 \text{ wt } \%$ AIBN is introduced in the reactor under pressure using a syringe pump (100DX, ISCO Inc.). The final ratio of AIBN/MMA is $1 \text{ wt } \%$ for all the experiments. At the end of the reaction, the reactor content is quenched by cooling and by venting CO_2 through a discharge tube. The polymer powder is then collected in the reactor after opening the reactor. Global product yield and the quantity of PDMS monomethacrylate chemically incorporated in the final product are evaluated gravimetrically. Extraction experiments of PDMS macromonomer with hexane (Reactolab SA, Switzerland) are carried out to distinguish between the amounts of PDMS monomethacrylate physically and chemically incorporated in the final product. After drying the polymer, four samples (0.2 g) of each experiment are

(12) Wilson, E. E. *Am. Soc. Mech. Eng.* **1915**, 37, 47.

(13) Brooks, G.; Su, G.-J. *Chem. Eng. Prog.* **1959**, 55, 54.

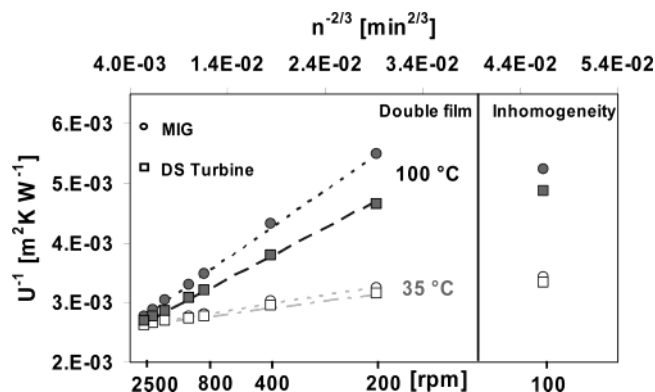


Figure 5. Wilson plots for the double-stage turbine and the MIG, scCO₂ density of 430 kg/m³.

prepared in small test tubes for centrifugation and left under stirring with hexane for 1 h and then centrifuged for 15 min at 9000 rpm. The solution of hexane containing the extracted PDMS macromonomer is removed carefully, and the samples are dried. It is possible to calculate the amount of PDMS macromonomer chemically incorporated in the final product from the mass balance for the dried product. The polymer is characterized in terms of molecular weight by triple detection size exclusion chromatography (TDA 300, Viscotek), particle size distribution (Mastersizer2000, Malvern Instruments), and morphology by electron microscopy (SEM).

Results and Discussions

The global heat transfer coefficient could be measured (Figure 5) using a calibration probe in the system delivering a known amount of power (25 W) using eq 4.

The linear plot in Figure 5 thus confirms that raising to the 2/3 power is still valid with supercritical carbon dioxide for the two agitators. This linear trend clearly indicates that the global heat transfer coefficient completely follows the Wilson plot regression at all temperatures and scCO₂ densities, except for 100 rpm stirrer speed where the system is inhomogeneous due to insufficient stirring. Moreover, the fact that the regression line of the turbine is below the one for the MIG shows that, in terms of heat transfer, the turbine is more efficient than the MIG at the given temperatures. At 35 °C the intrinsic properties of scCO₂ such as heat conductivity and heat capacity drastically improve. This means that h_t values increase and explains why the difference between MIG and turbine regression lines becomes smaller as they converge to the external film resistance $1/\varphi$ value.

Another fundamental conclusion is that the behaviour of the internal heat transfer coefficient h_t is inverse to the one observed for classical liquid systems. The slope of the Wilson plot regression lines allows for the calculation of this internal film coefficient. The intercept with the U axis (meaning infinite rotation speed) determines the global heat transfer coefficient of the external part φ taken from eq 8. It comes out that the regression lines cross before the U axis, indicating that the external film behaviour is exactly opposite to that of the internal film with respect to temperature. This tendency clearly shows the accuracy of the experiments, as it demonstrates that, independently on the media, the external

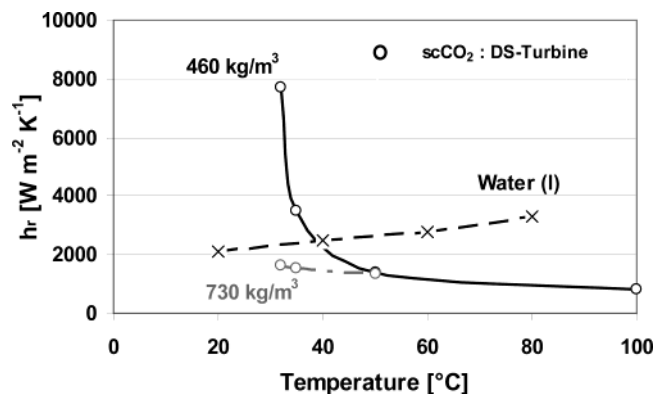


Figure 6. Experimental internal heat transfer coefficient for two scCO₂ densities and liquid water.

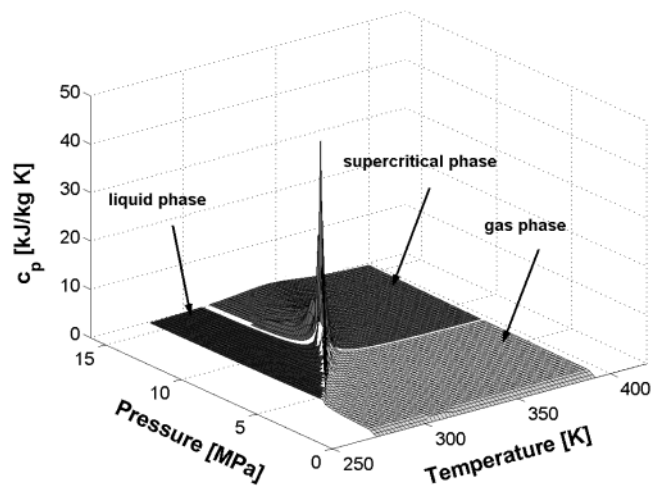


Figure 7. Three-dimensional view of a P – T – c_p phase diagram for carbon dioxide.⁵

heat transfer coefficient part, which includes conduction through the vessel wall and transfer through the stagnant coolant film, is improving with temperature. This effect is mainly due to the decrease of the coolant viscosity with temperature.

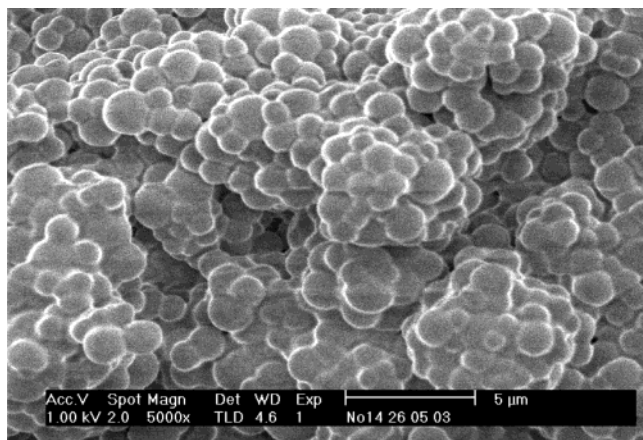
The experimental behaviour of h_t is presented in Figure 6 which compares experimental h_t for a classical liquid (water) and scCO₂ at 400 rpm with the two-stage turbine.

The internal heat transfer coefficient improves asymptotically close to the critical point for scCO₂. This tendency is drastically opposite to that of water where h_t is improving quite linearly with the temperature.

To understand why this particular behaviour occurs with scCO₂, we take another look at eq 9. The correlation of the Nusselt number relates the internal film coefficient with the Reynolds number raised to the 2/3 power and to the Prandtl number raised to the 1/3 power. The quantities c_p , λ , and μ in eq 9 are those of interest, the other parameters being constant with temperature. In fact, the strange behaviour of h_t for scCO₂ is mainly due to the behaviour of those three quantities. As illustration, the asymptotic critical divergence of the c_p values near the critical point (i.e. near P_c , T_c , and the critical density), are depicted in Figure 7.⁵ Due to this divergence, c_p values can easily rise by 2 orders of magnitude close to the critical point. This effect happens also for the thermal conductivity λ of scCO₂ and the viscosity μ as shown

Table 1. Experimental conditions and results of the dispersion polymerizations

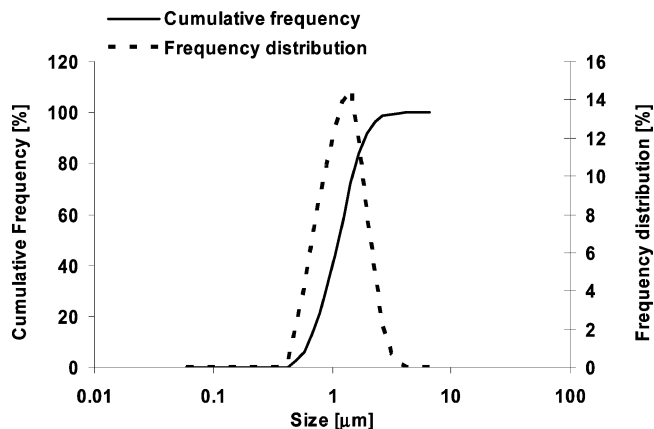
entry	P_0 [bar]	P_r [bar]	yield [%]	M_w [kg/mol]	PDI [-]	d_p (SEM) [μm]	$D(v,0.9)$ [μm]	span [-]	wt % PDMS incorporated
1	228	262	94	119	2.3	1.2–2.3	1.9	1.1	4.8
2	223	268	95	126	2.2	—	2.1	1.1	4.3

**Figure 8.** SEM micrographs of PMMA produced at 600 rpm.

by Vesovic et al. but with a smaller magnitude especially for the viscosity.¹⁴ The combination of the diverging behaviour of λ and c_p explains the behaviour of the internal heat transfer coefficient h_r as this last is proportional to $\lambda^{2/3}$ and $c_p^{1/3}$ and is thus submitted to the same asymptotic divergence in the vicinity of the critical point.¹⁵ h_r is also inversely proportional to viscosity μ raised to the 1/3 power. Viscosity shows some divergence around the critical point, but in contrast to heat conductivity, μ has a very short range of densities where critical enhancement is significant and moreover at temperature very close to the critical one (less than 1 °C).

The preliminary results for the methyl methacrylate polymerization in supercritical CO₂ using commercially available stabilizers are presented in Table 1. To test the reproducibility, several experiments are performed under the same conditions: i.e., 10% (wt) PDMS/MMA and 600 rpm stirring with the Ekato MIG.

The characteristic polymerization time was 150 min, and the reaction temperature was maintained at 80 °C. In Table 1, P_0 corresponds to the pressure of the reactor before adding the mixture of MMA and AIBN, i.e., before the beginning of the polymerization. P_r corresponds to the pressure at the end of the polymerization reaction. This pressure increase is partially due to the added solution of MMA but mainly due to the polymerization reaction itself. The two experiments yield a fine white powder with high-molecular weight at monomer conversions higher than 90% and a well-defined spherical morphology observable by SEM micrograph (Figure 8). Molecular weights are lower than the ones published by Giles et al. where the experiments were realized in the absence of stirring.¹⁶ The quantity of PDMS macromonomer

**Figure 9.** Particle size distribution of the polymerization no. 1.

chemically incorporated is between 4 and 5% of total mass with a high reproducibility.

Using the particle sizer instrument for particle characterization allows the sample identification by its particle size distribution. This information is generally used by manufacturers to guarantee the specification of powders. The distribution function term $D(v,0.9)$ in Table 1 means that 90% of the particles have a diameter under the given value. Figure 9 shows typical particle size distributions obtained for the polymerization no. 1.

Moreover, in Table 1 the span term gives an indication of the width of particle size distribution and is given by:

$$\text{Span} = \frac{D(v,0.9) - D(v,0.1)}{D(v,0.5)} [-] \quad (10)$$

At commercial scale, stirring is essential to ensure thermal homogeneity and to avoid thermal runaway. Using 10 wt % PDMS stabilizer, the dispersion polymerization of MMA in scCO₂ can be performed under efficient stirring.

The overall heat transfer coefficient was measured before the addition of the AIBN/MMA solution (e.g., in absence of any reaction) and at the end of the polymerization. The next challenge will be to develop a methodology to allow the accurate measurement of the overall heat transfer coefficient according to the evolving physical and chemical properties.

It was observed that the heat released by the polymerization reaction is dependent on the stabilizer concentration since the latter has a direct influence on the stability of the dispersion and hence on the MMA conversion. First trials with 5 wt % stabilizer induced a low reaction rate and less effective stabilized polymerization. The thermal signal was too close to the baseline, i.e. at the limit of the sensitivity of the apparatus, preventing a good heat balance evaluation. The two experiments are very reproducible in terms of heat flux as depicted in Figure 10. By integration of the thermal

(14) Vesovic, V.; Wakeham, W. A.; Olchowky, G. A.; Sengers, J. V.; Watson, J. T. R.; Millat, J. *J. Phys. Chem. Ref. Data* **1990**, *19*, 763.

(15) Lavanchy, F.; Fortini, S.; Meyer, T. J. *Supercrit. Fluid* To be published.

(16) Giles, M. R.; Hay, J. N.; Howdle, S. M.; Winder, R. J. *Polymer* **2000**, *41*, 6715.

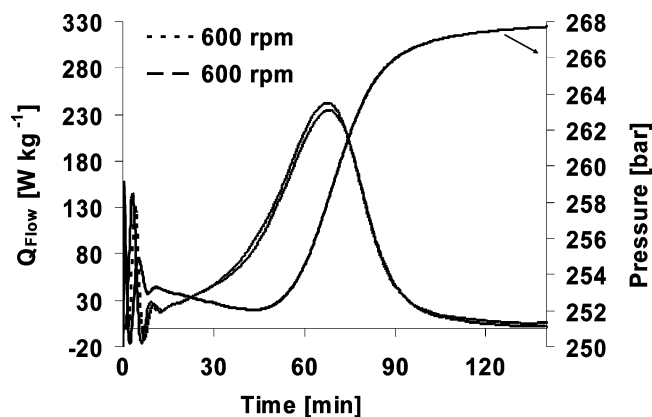


Figure 10. Heat flow production of the dispersion polymerization of MMA in scCO_2 , $T_r = 80^\circ\text{C}$ and AIBN/MMA = 1 wt %.

curves, the enthalpy of polymerization could be calculated using eq 7.

The measured value $-58.8 \pm 3 \text{ kJ/mol}$ is in good agreement with the literature value of -57.8 kJ/mol for conventional solvents.¹⁷ This important result shows the potential of reaction calorimetry for determining kinetic and thermodynamic data for supercritical fluid processes. Despite the high reproducibility of both experiments, the uncertainty of 3 kJ/mol on the enthalpy value corresponds mainly to the integration method employed (i.e., selected baseline, UA values utilization, etc.).

Conclusions

This new supercritical calorimeter system allows the evaluation of calorimetric measurements under supercritical conditions which is definitely not trivial. However, the complex phenomena of heat transfer with SCFs should be carefully taken into account to be able to proceed with correct chemical reactions evaluation.

(17) Brandrup, J.; Immergut, E. H. *Polymer Handbook*, 3rd ed.; John Wiley & Sons: New York, 1989.

Some preliminary results with the so-called “supercritical reaction calorimetry” field have been presented: the Wilson Plot analysis and the dispersion polymerization reaction of methyl methacrylate in scCO_2 . The Wilson plot study allowed the understanding of the fundamental behaviour of the internal film coefficient, which does not follow the same tendency as for classical liquids with respect to temperature, due to the very specific properties of scCO_2 near its critical point. On the other hand, the linear trends of the Wilson plot regressions confirm the value of the Reynolds number raised to the 2/3 power in the Nusselt expression.

Furthermore, it has been shown that poly(dimethylsiloxane) monomethacrylate with a molecular weight of 5000 g/mol is a suitable stabilizer for the dispersion polymerization of methyl methacrylate in supercritical carbon dioxide under efficient stirring. The studied polymerization is taken as model reaction for the development of supercritical reaction calorimetry. The measured enthalpy of polymerization is in good agreement with previously reported data. The high reproducibility indicates that the reaction calorimeter operates accurately.

However, the realization of supercritical polymerization calorimetry is characterized by several technical difficulties. Most of the complications are related to the fact that the physicochemical properties of the reaction medium change during the polymerization. This implies, for example, that the evolution of the overall heat transfer coefficient during the reaction has to be taken into account as well as the heat input dissipated by the stirrer.

Acknowledgment

The “Fonds National Suisse pour la Recherche” No. 21.61403.00 is gratefully acknowledged for its financial support.

Received for review November 27, 2003.

OP034174N